Supplementary Information for

Real-time exchange of the lipid-bound intermediate and post-fusion states of the HIV-1 gp41 ectodomain

Sai Chaitanya Chiliveri, John M Louis, Robert Best and Ad Bax*

Laboratory of Chemical Physics, National Institute of Diabetes and Digestive and Kidney Diseases, National Institutes of Health, Bethesda, MD 20892, USA.

*Corresponding author. Email: bax@nih.gov

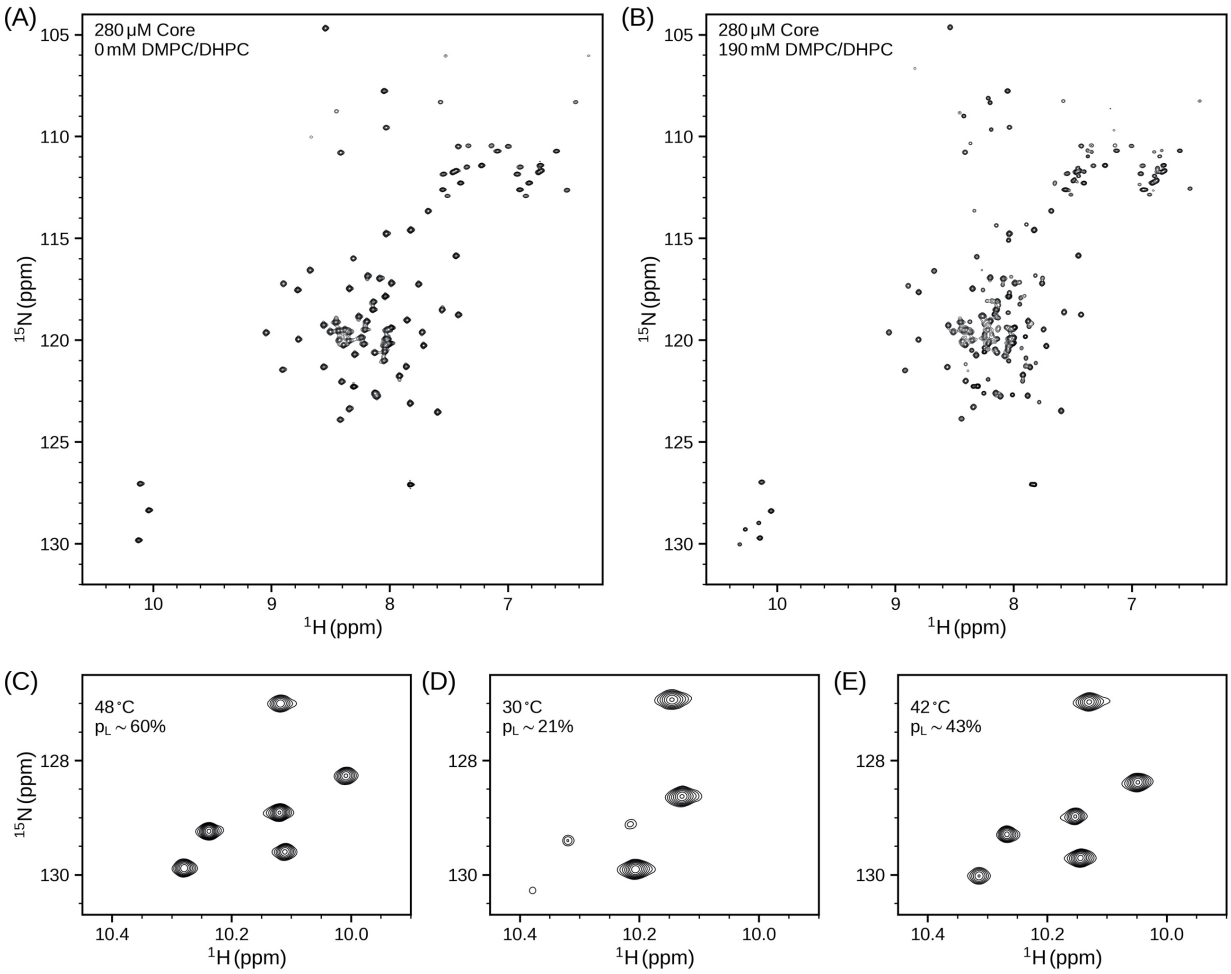

Figure S1. Dissociation of gp41-Core in the presence of phospholipid bicelles. ^{1}H-^{15}N HSQC NMR spectra (800 MHz) of 280 µM [^{13}C/^{15}N/^{2}H]-Core in (A) the absence and (B) the presence of 190 mM DMPC/DHPC at 42 °C and pH 6. New resonances that are only seen in the presence of bicelles correspond to the lipid-bound state of Core. Excerpts from ^{1}H-^{15}N HSQC spectra at (C) 48 °C, (D) 30 °C and (E) 42 °C. Population of the lipid-bound state (p_L) was decreased from 60% (at 48 °C) to 31% (at 30 °C), followed by an increase to 43% (at 42 °C), exemplifying reversibility of the equilibrium.

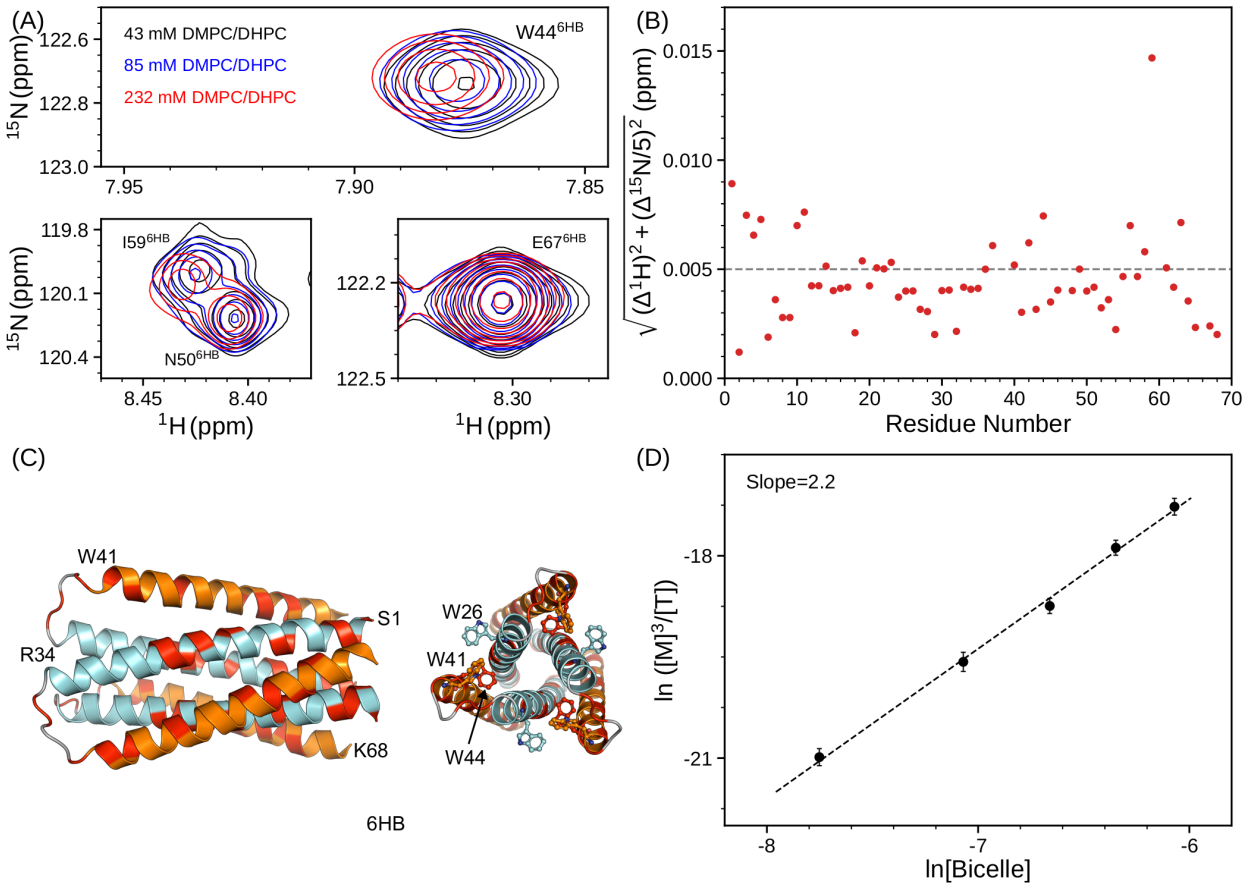

Figure S2. Characterization of gp41 Core 6HB dissociation. (A) Overlay of small regions of ^{1}H-^{15}N HSQC spectra of Core (280 μM) with 43 mM (black), 85 mM (blue) and 232 mM DMPC/DHPC (red). Small chemical shift changes for W44 and I59 in the 6HB state suggest its transient interaction with bicelles. The 6HB state of E67 does not experience significant chemical shift changes. (B) Normalized Core chemical shift changes in the presence of 43 mM and 232 mM DMPC/DHPC. (C) Residues that exhibit more than 0.005 ppm changes (from panel B) are displayed in red on the 6HB structure. (D) Linear regression for the fraction of lipid-bound and 6HB state, ln ($[M]^3/[T]$), against bicelle concentration, ln[Bicelle]. Bicelle concentration was re-calculated by assuming that 100 lipids constitute a single bicelle particle.[1] A slope of ca. 2.2 suggests that 2 bicelles are required for 6HB dissociation into monomers.

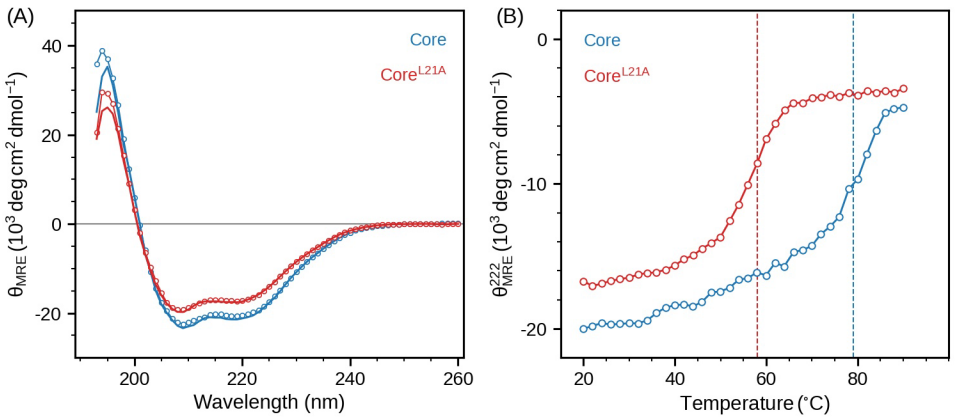

Figure S3. Stability of gp41-Core and Core^{L21A} in aqueous solution. Overlay of far-UV CD spectra of 17 μM Core (blue) and 30 μM Core^{L21A} (red) at 35 °C in buffer A. (B) Thermal melting of Core and Core^{L21A} as a function of temperature. Melting temperatures (T_m) of Core and Core^{L21A} are 79 °C and 58 °C, respectively. CD spectra for Core and Core^{L21A} after cooling down to 35 °C from 90 °C are shown in solid lines in the panel-(A). Both constructs contain an N-terminal His_6 tag.

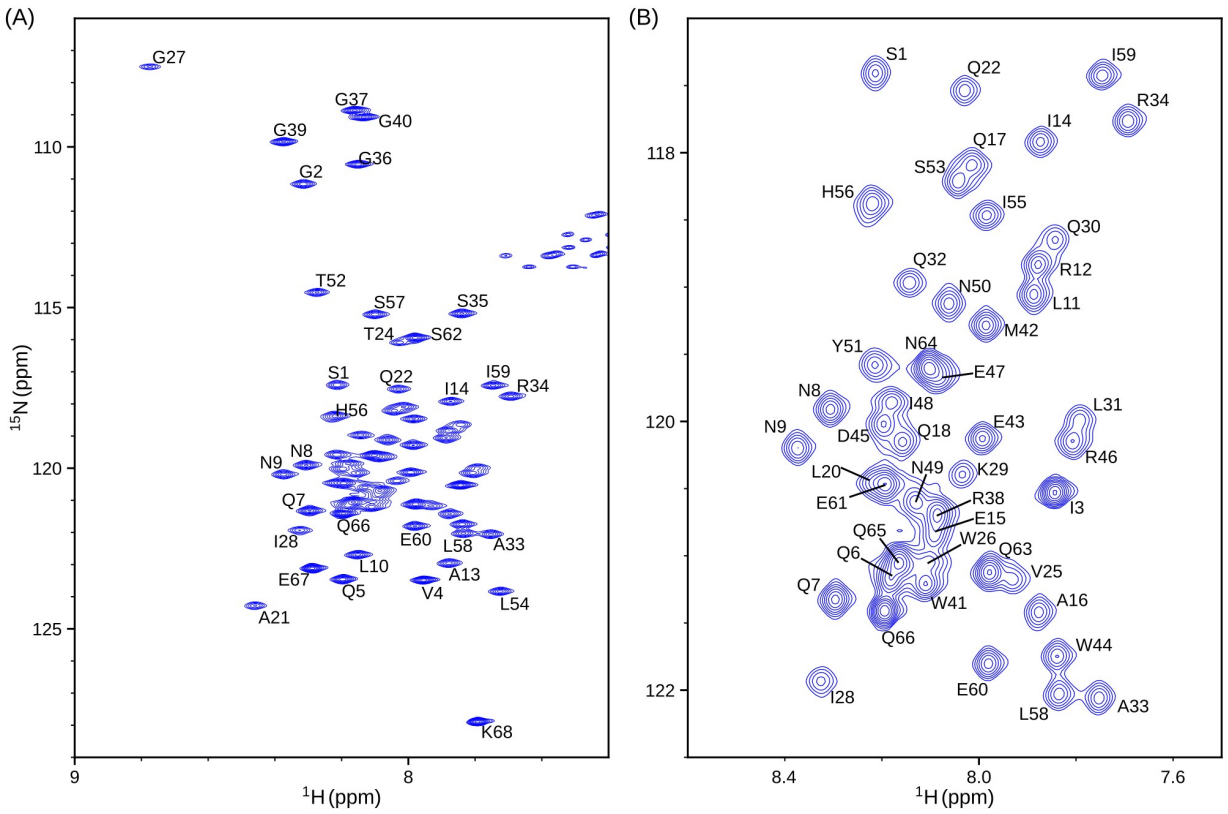

Figure S4. Bicelle-bound state of Core^{L21A}. (A) 700 MHz ^{1}H-^{15}N TROSY-HSQC spectrum showing chemical shifts assignments of Core^{L21A} in the lipid-bound state. (B) Expanded central region of panel A. Data collected at 40 °C for 200 µM Core^{L21A} in buffer A, additionally containing 200 mM DMPC/DHPC.

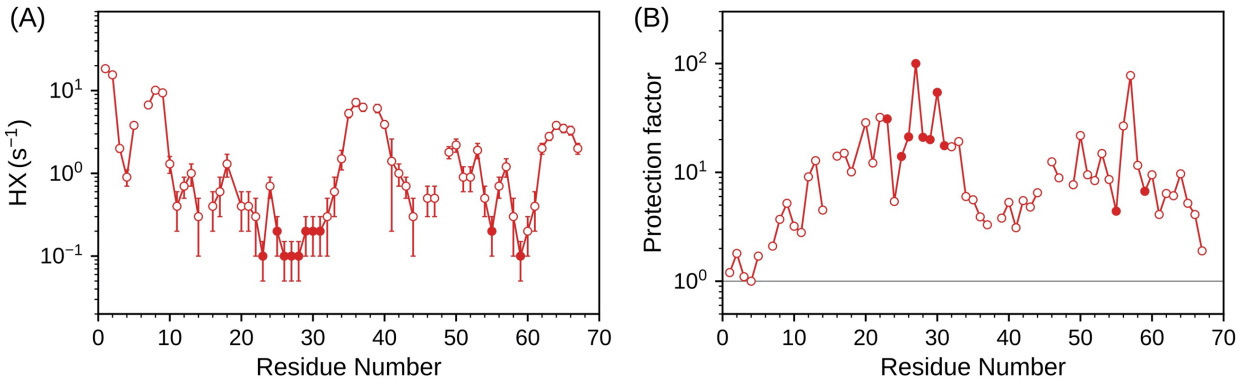

Figure S5. Hydrogen exchange of bicelle-bound Core^{L21A}. (A) Residue-specific hydrogen exchange rates (HX) and their corresponding (B) protection factors of Core^{L21A} normalized to pH 6.1. A protection factor of 1 (grey line) corresponds to no protection from hydrogen exchange, i.e., no significant population of intramolecular hydrogen bonds. Upper bound K_{ex} values, reported for a few residues that exchanged too slowly for accurate measurement, are shown as filled circles. Data obtained on 200 μM [^{15}N/^{2}H]-Core^{L21A} in buffer A containing 200 mM DMPC/DHPC bicelles at 40 °C on a 700 MHz spectrometer.

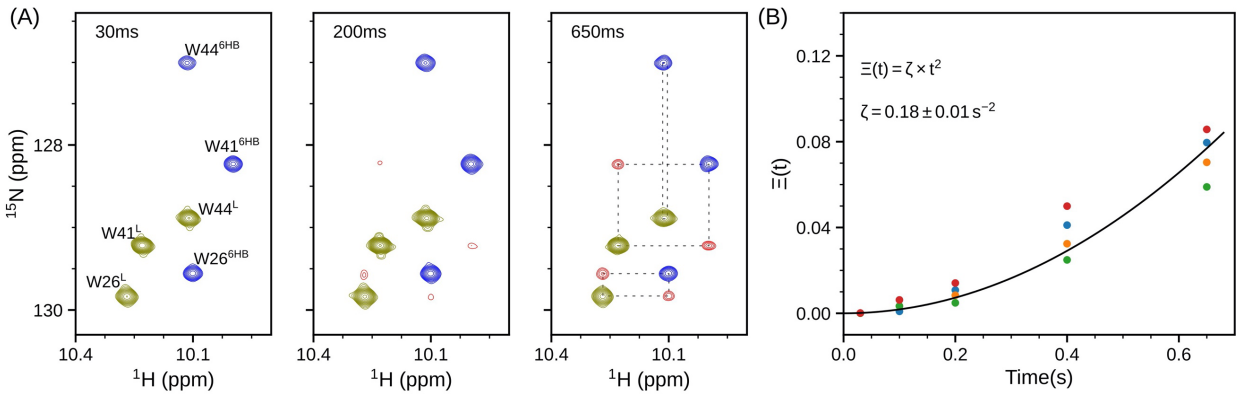

Figure S6. Slow exchange kinetics observed for wild-type Core. (A) Spectral region of Core showing Trp indole resonances at three different ^{15}N-ZZ mixing times (30 ms, 200 ms and 650 ms). Auto-correlation peaks for 6HB and bicelle-bound states are shown in blue and olive, respectively. Cross-peaks depicting exchange between the two states are shown in red. Cross peaks for W44 overlap with their autocorrelation resonances. (B) Global fit of the composite intensity ratio, Ξ(t), for four well-separated resonances (W26, W41, L54, and S57). Data obtained for 280 µM Core in buffer A, containing 190 mM DMPC/DHPC at 50 °C, 800 MHz.

Supplementary Table S1. $^{1}H^{N}$, ^{15}N, $^{13}C'$ and C^{α} chemical shifts of $Core^{L21A}$. Data collected at 700 MHz, 40 °C, on 200 μM [$^{13}C/^{15}N$] $Core^{L21A}$ in buffer A, containing 200 mM DMPC/DHPC. $\Delta\delta^{13}C'$ and $\Delta\delta^{13}C^{\alpha}$ are the deviations of $^{13}C'$ and $^{13}C^{\alpha}$ chemical shifts from neighbor-corrected random coil chemical shifts.[2]

Residue	Name	$^{1}H^{N}$ (ppm)	^{15}N (ppm)	$^{13}C'$ (ppm)	$^{13}C^{\alpha}$ (ppm)	$\Delta\delta^{13}C'$ (ppm)	$\Delta\delta^{13}C^{\alpha}$ (ppm)
1	SER	8.213	117.409	175.08	58.91	0.27	0.35
2	GLY	8.315	111.157	174.39	45.71	1.08	0.37
3	ILE	7.843	120.530	176.53	61.86	0.21	0.81
4	VAL	7.954	123.485	176.47	63.28	0.56	0.96
5	GLN	8.196	123.460	176.42	56.66	0.68	0.75
6	GLN	8.182	121.163	176.46	56.60	0.54	0.48
7	GLN	8.296	121.325	176.06	56.75	0.35	0.57
8	ASN	8.306	119.910	175.80	54.25	0.97	0.60
9	ASN	8.374	120.198	176.59	54.90	1.59	1.34
10	LEU	8.151	122.693	177.84	57.57	0.60	2.10
11	LEU	7.887	119.055	178.65	57.33	1.48	2.08
12	ARG	7.878	118.833	178.13	58.18	2.49	2.34
13	ALA	7.878	122.956	179.15	54.61	1.69	2.33
14	ILE	7.873	117.919	177.44	63.83	1.26	2.64
15	GLU	8.091	120.833	178.00	58.68	1.85	2.22
16	ALA	7.877	121.420	178.81	54.41	1.13	1.78
17	GLN	8.014	118.091	177.24	57.79	1.26	1.77
18	GLN	8.157	120.153	178.00*	58.68	2.43*	2.51
19	HIS	8.307*	117.964*	177.25	58.10*	3.04	2.67*
20	LEU	8.217	120.466	179.41	57.85	2.49	2.65
21	ALA	8.459	124.281	179.24	55.80	1.78	3.09
22	GLN	8.029	117.538	179.00	59.02	3.15	3.22
23	LEU	8.145	121.081	178.37	58.01	1.09	2.77
24	THR	8.026	116.09	175.93	67.66	1.59	5.89
25	VAL	7.932	121.173	177.55	67.09	1.82	4.52
26	TRP	8.105	121.051	178.50	61.74	2.34	4.48
27	GLY	8.774	107.507	174.95	47.64	1.67	2.26
28	ILE	8.326	121.933	177.94	65.30	1.63	4.12
29	LYS	8.034	120.395	179.80	59.63	3.61	3.19
30	GLN	7.843	118.648	178.41	57.66	2.68	1.83
31	LEU	7.793	119.995	179.00	57.49	1.79	2.03
32	GLN	8.143	118.968	177.73	58.28	2.17	2.45

33	ALA	7.753	122.058	178.90	53.89	1.21	1.38
34	ARG	7.693	117.765	176.72	56.60	0.32	0.52
35	SER	7.840	115.185	175.21	59.20	0.08	0.64
36	GLY	8.150	110.540	174.82	45.77	0.76	0.19
37	GLY	8.160	108.863	174.33	45.53	0.58	0.17
38	ARG	8.086	120.699	176.83	56.33	-0.19	-0.05
39	GLY	8.374	109.842	174.56	45.52	0.79	0.18
40	GLY	8.134	109.071	174.44	45.55	0.87	0.27
41	TRP	8.110	121.207	176.54	58.19	0.32	0.87
42	MET	7.985	119.285	176.57	56.74	0.91	1.21
43	GLU	7.993	120.127	177.07	57.05	0.81	-0.07
44	TRP	7.839	121.747	176.45	58.60	0.78	1.21
45	ASP	8.196	120.019	177.26	56.22	1.64	1.92
46	ARG	7.807	120.147	177.78	58.18	1.62	1.83
47	GLU	8.082	119.687	178.14	58.12	1.57	1.49
48	ILE	8.180	119.858	177.56	63.67	1.68	2.37
49	ASN	8.130	120.600	176.70	55.48	1.98	1.98
50	ASN	8.062	119.123	177.01	55.22	2.17	1.56
51	TYR	8.214	119.580	177.45	60.90	1.62	2.93
52	THR	8.274	114.529	176.69	66.42	2.73	4.45
53	SER	8.043	118.212	176.75	61.57	2.55	3.24
54	LEU	7.725	123.838	178.93	58.08	1.83	2.89
55	ILE	7.984	118.466	177.38	64.52	1.48	3.41
56	HIS	8.219	118.378	176.82	59.44	2.72	3.81
57	SER	8.100	115.215	175.66	61.64	1.59	3.45
58	LEU	7.835	122.028	178.52	57.32	1.43	2.08
59	ILE	7.746	117.425	177.39	63.33	1.35	2.22
60	GLU	7.980	121.803	177.74	58.19	1.33	1.63
61	GLU	8.194	120.467	177.58	57.69	0.94	0.93
62	SER	7.980	115.943	175.08	59.78	0.36	1.25
63	GLN	7.978	121.123	176.09	56.28	0.35	0.08
64	ASN	8.102	119.606	175.33	53.61	0.08	0.02
65	GLN	8.165	121.054	175.88	56.12	0.03	-0.13
66	GLN	8.194	121.410	175.86	56.05	-0.14	-0.15
67	GLU	8.288	123.119	175.40	56.08	-1.09	0.13
68	LYS	7.792	127.894	-	57.66	-	-0.22

*His19 resonance is severely broadened at pH 6 and reported values correspond to pH 5.4.

Supplementary Table S2. Hydrogen exchange rates (HX) for 200 μM [$^{15}N/^{2}H$]-Core^{L21A} in buffer A containing 200 mM DMPC/DHPC at 40 °C on a 700 MHz spectrometer. Values of HX and protection factors are normalized to pH 6.1.

Residue Number	Name	HX (s^{-1})	error (s^{-1})	Protection factor
1	SER	18.4	1.5	1.2
2	GLY	15.5	1.3	1.8
3	ILE	2.0	0.2	1.1
4	VAL	0.9	0.2	1.0
5	GLN	3.8	0.3	1.7
6	GLN	-	-	-
7	GLN	6.7	0.4	2.1
8	ASN	10.1	0.6	3.7
9	ASN	9.4	0.5	5.2
10	LEU	1.3	0.3	3.2
11	LEU	0.4	0.2	2.8
12	ARG	0.7	0.2	9.1
13	ALA	1.0	0.3	12.8
14	ILE	0.3	0.2	4.5
15	GLU	-	-	-
16	ALA	0.4	0.2	14.1
17	GLN	0.6	0.3	15.0
18	GLN	1.3	0.4	10.1
19	HIS	-	-	-
20	LEU	0.4	0.2	28.6
21	ALA	0.4	0.2	12.2
22	GLN	0.3	0.2	32.0
23	LEU	<0.1	0.1	>31.0
24	THR	0.7	0.2	5.4
25	VAL	<0.2	0.1	>14.0
26	TRP	<0.1	0.1	>21.2
27	GLY	<0.1	0.1	>100.0
28	ILE	<0.1	0.1	>21.0
29	LYS	<0.2	0.1	>20.0
30	GLN	<0.2	0.1	>54.3
31	LEU	<0.2	0.1	>17.6
32	GLN	0.3	0.2	17.2
33	ALA	0.6	0.3	19.2
34	ARG	1.5	0.4	6.0

35	SER	5.3	0.6	5.6
36	GLY	7.2	0.8	3.9
37	GLY	6.3	0.7	3.3
38	ARG	-	-	-
39	GLY	6.1	0.7	3.8
40	GLY	3.9	0.4	5.3
41	TRP	1.4	1.2	3.1
42	MET	1.0	0.3	5.5
43	GLU	0.7	0.2	4.8
44	TRP	0.3	0.2	6.5
45	ASP	-	-	-
46	ARG	0.5	0.2	12.5
47	GLU	0.5	0.2	8.9
48	ILE	-	-	-
49	ASN	1.8	0.3	7.7
50	ASN	2.2	0.4	21.8
51	TYR	0.9	0.3	9.5
52	THR	0.9	0.3	8.4
53	SER	1.9	0.4	14.9
54	LEU	0.5	0.2	8.6
55	ILE	<0.2	0.1	>4.4
56	HIS	0.7	0.2	26.7
57	SER	1.2	0.3	77.6
58	LEU	0.3	0.2	11.6
59	ILE	<0.1	0.1	>6.7
60	GLU	0.2	0.1	9.5
61	GLU	0.4	0.2	4.1
62	SER	2.0	0.3	6.4
63	GLN	2.8	0.3	6.1
64	ASN	3.8	0.4	9.7
65	GLN	3.5	0.4	5.2
66	GLN	3.3	0.4	4.1
67	GLU	2.0	0.3	1.9

Supplementary Table S3. ^{15}N-{^{1}H} NOE values of Core^{L21A} in the 6HB and bicelle-bound states measured at 600 MHz. Uncertainties in these measurements, derived from the signal to noise ratio, are 0.03. [c]

Number	Name	NOE[a]	NOE[b]
1	SER	0.39	-0.27
2	GLY	0.44	-0.23
3	ILE	0.52	-0.08
4	VAL	0.69	-0.16
5	GLN	0.63	-0.11
6	GLN	0.70	-
7	GLN	0.69	0.04
8	ASN	-	0.19
9	ASN	0.80	0.26
10	LEU	0.88	0.36
11	LEU	0.79	0.36
12	ARG	0.81	0.50
13	ALA	0.82	0.51
14	ILE	0.77	0.56
15	GLU	0.89	-
16	ALA	0.81	0.50
17	GLN	0.78	0.55
18	GLN	0.81	0.57
19	HIS	0.84	-
20	LEU	0.85	0.57
21	ALA	0.83	0.56
22	GLN	-	0.56
23	LEU	0.83	0.58
24	THR	0.82	0.60
25	VAL	0.84	0.68
26	TRP	0.82	0.63
27	GLY	0.87	0.74
28	ILE	0.86	0.72
29	LYS	0.83	0.69
30	GLN	0.80	0.60
31	LEU	0.87	0.62
32	GLN	0.81	0.53
33	ALA	0.63	0.52
34	ARG	0.55	0.45
35	SER	0.47	0.36

36	GLY	0.24	0.27
37	GLY	-	0.22
38	ARG	-	-
39	GLY	-	0.20
40	GLY	0.53	0.29
41	TRP	0.53	0.41
42	MET	0.74	0.52
43	GLU	0.68	0.41
44	TRP	0.77	0.50
45	ASP	0.81	-
46	ARG	0.74	0.49
47	GLU	0.71	0.48
48	ILE	0.81	-
49	ASN	0.80	0.52
50	ASN	0.81	0.57
51	TYR	0.83	0.57
52	THR	0.83	0.61
53	SER	0.82	0.64
54	LEU	0.81	0.58
55	ILE	0.77	0.58
56	HIS	0.75	0.61
57	SER	0.81	0.59
58	LEU	0.81	0.57
59	ILE	0.78	0.52
60	GLU	0.73	0.48
61	GLU	0.67	0.32
62	SER	0.60	0.21
63	GLN	0.58	0.12
64	ASN	0.49	-0.05
65	GLN	0.27	-0.33
66	GLN	0.15	-
67	GLU	-0.01	-0.86
68	LYS	-0.36	-1.40

[a] for 6HB state

[b] for bicelle-bound state

[c] Data obtained on 200 μM [$^{15}N/^{2}H$]-Core^{L21A} in buffer A at 40 °C, in the absence and presence of 200 mM DMPC/DHPC

References

[1] Situ, A. J., Schmidt, T., Mazumder, P. & Ulmer, T. S. (2014). Characterization of membrane protein interactions by isothermal titration calorimetry. *J. Mol. Biol.* **426**, 3670–3680.

[2] Kjaergaard, M., Brander, S. & Poulsen, F. M. (2011). Random coil chemical shift for intrinsically disordered proteins: Effects of temperature and pH. *J. Biomol. NMR* **49**, 139–149.